

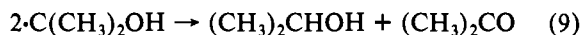
the determination of k_5 is based on small differences. Thus a series of determinations using a high and constant concentration of chromium(III) ions, 6.96×10^{-2} M, and a constant reaction medium (0.200 M perchloric acid, 1.13 M 2-propanol) was carried out. The principal variable was $[\text{Cr}^{2+}]$, ranging between 1.8×10^{-4} and 3.0×10^{-3} . The kinetic data are as follows, where k_5 was calculated by using $k_A = 4.30 \times 10^{-3} \text{ s}^{-1}$:

$[\text{Cr}^{2+}]/\text{M}$	$k_{\text{obsd}}/\text{s}^{-1}$	$k_5/(\text{M}^{-1} \text{ s}^{-1})$
1.8×10^{-4}	4.75×10^{-3}	4.13×10^2
8.8×10^{-4}	4.46×10^{-3}	6.0×10^2
2.96×10^{-3}	4.38×10^{-3}	6.8×10^2
		av $(5.6 \pm 1.4) \times 10^2$

The very low rate constant of the reaction of eq 5 could have previously been inferred since it is never a factor in other competition or kinetic experiments involving $\text{CrC}(\text{CH}_3)_2\text{OH}^{2+}$ in solutions containing low but variable concentrations of $\text{Cr}(\text{H}_2\text{O})_6^{3+}$.

Europium-Catalyzed Disproportionation of $\cdot\text{C}(\text{CH}_3)_2\text{OH}$

The summation of eq 3 and 4 is equivalent to disproportionation of the aliphatic radicals, eq 9. This spontaneous reaction



has a very high rate constant, $k_9 = 6.5 \pm 0.5 \times 10^9 \text{ M}^{-1} \text{ s}^{-1}$,¹⁷ but is not important as a direct reaction in this work owing to the low concentration of the free radical which prevails throughout.

On the other hand, the sequential occurrence of the two reactions noted, eq 3 and 4, leads to the same overall net reaction; if it occurs to a major extent it would then constitute a europium-catalyzed pathway for free-radical disproportionation. Reaction conditions were selected to minimize its importance. In retrospect, the easiest way to gauge the success of the experimental control is to examine the summation $k_3[\text{Eu}^{3+}] + k_4[\text{Eu}^{2+}]$, which would be the catalyzed rate constant. In experiments dealing with reaction 4 (Table II), the first term never contributes more than 6.0% to the sum. In the Eu^{3+} experiments (Table I), the second term never amounts

to more than 10.1%. Both figures apply at the midpoint of the kinetic runs. It is clear from this analysis that the catalyzed disproportionation reaction does not make an appreciable contribution under the concentration conditions used for kinetic evaluations.

Discussion

Reaction Mechanisms. The rate constants for the reactions in which $\text{Eu}(\text{aq})^{3+}$ and $\text{Cr}(\text{H}_2\text{O})_6^{3+}$ are reduced by $\cdot\text{C}(\text{CH}_3)_2\text{OH}$ differ by a factor of nearly 10^2 . A similar qualitative difference was found¹ in comparing the ready reaction of $\cdot\text{CO}_2/\cdot\text{COOH}$ with Eu^{3+} under conditions where Cr^{3+} does not react. An outer-sphere electron transfer mechanism is often assigned to reactions in which $\cdot(\text{CH}_3)_2\text{OH}$ functions as a reducing agent. Alternatively electron transfer may occur within a charge-transfer complex. The lower reactivity of Cr^{3+} may well be a consequence of a slower self-exchange for $\text{Cr}^{3+}/\text{Cr}^{2+}$ as compared to $\text{Eu}^{3+}/\text{Eu}^{2+}$ and to the much greater tendency for the latter to involve major contributions from nonadiabaticity. Similar arguments have been advanced¹⁸ to account for the differences in the solvent isotope effects for the electrochemical self-exchange rate constants for $\text{Cr}^{3+}/\text{Cr}^{2+}$ as compared to $\text{Eu}^{3+}/\text{Eu}^{2+}$.

The oxidation of $\text{Eu}(\text{aq})^{2+}$ by $\cdot\text{C}(\text{CH}_3)_2\text{OH}$ appears, like the oxidation of $\text{V}(\text{H}_2\text{O})_6^{2+}$,³ to proceed by a hydrogen atom abstraction mechanism, as depicted in eq 10. Evidence for $\text{Eu}(\text{H}_2\text{O})_x^{2+} + \cdot\text{C}(\text{CH}_3)_2\text{OH} \rightarrow \text{EuOH}^{2+} + (\text{CH}_3)_2\text{CHOH}$ (10)

this consists, in part, of the large kinetic isotope effects, 4.8 for Eu^{2+} and 6.0 for V^{2+} (Table III). It is possible to account more quantitatively for the kinetic isotope effects found here in terms of isotope fractionation factor theory,^{15,19} but those results will be given elsewhere.²⁰

Acknowledgment. This work was supported by the U.S. Department of Energy, Office of Basic Energy Sciences, Chemical Sciences Division, under Contract W-7405-ENG-82.

Registry No. Europium, 7440-53-1; 2-hydroxy-2-propyl, 5131-95-3.

(17) Rabani, J.; Mulac, W. A.; Matheson, M. S. *J. Phys. Chem.* **1977**, *81*, 99. The rate law defining k_9 is $-d[\text{R}\cdot]/dt = 2k_9[\text{R}\cdot]^2$.

(18) Weaver, M. J.; Li, T. T. *J. Phys. Chem.* **1983**, *87*, 1153.

(19) Gold, V. *Adv. Phys. Org. Chem.* **1969**, *7*, 259.

(20) Muralidharan, S.; Espenson, J. H.; unpublished results.

Contribution from the Department of Chemistry, National Tsing Hua University, Hsinchu, Taiwan 300, Republic of China

Kinetics of Coordinated-Base-Catalyzed and Free-Base-Catalyzed Configurational Conversions of a Tetraamine Macrocyclic Ligand Complex of Copper(II)

CHUNG-SHIN LEE and CHUNG-SUN CHUNG*

Received April 29, 1983

In order to investigate the effect of coordinated hydroxide ion and free hydroxide ion in configurational conversion of a tetraamine macrocyclic ligand complex, the kinetics of the blue-to-red interconversion of the copper(II) complex of *meso*-5,5,7,12,12,14-hexamethyl-1,4,8,11-tetraazacyclotetradecane has been examined spectrophotometrically for $[\text{OH}^-]$ between 1.99×10^{-4} and 5.00 M. All the data are satisfactorily fitted by the rate law $R = (k_1 K_{\text{OH}}[\text{OH}^-] + k_2 K_{\text{OH}}[\text{OH}^-]^2)(1 + K_{\text{OH}}[\text{OH}^-])^{-1}([\text{Cu}(\text{tet a})(\text{blue})]^{2+} + [\text{Cu}(\text{tet a})(\text{OH})(\text{blue})]^{+})$, with $k_1 = 5.51 \text{ s}^{-1}$, $k_2 = 0.84 \text{ M}^{-1} \text{ s}^{-1}$, and $K_{\text{OH}} = 51.6 \text{ M}^{-1}$ at 25.0 °C and $\mu = 5.0 \text{ M}$ ($\text{NaNO}_3 + \text{NaOH}$). The ΔH^\ddagger and ΔS^\ddagger values for k_1 are 10.8 kcal mol⁻¹ and -19.0 eu, respectively. These small ΔH^\ddagger and negative ΔS^\ddagger values suggest a concerted coordinated-base-catalyzed mechanism in which intramolecular hydrogen bonding, nitrogen inversion, solvation, and ring conformational changes occur. The ΔH^\ddagger and ΔS^\ddagger values for k_2 are 22.8 kcal mol⁻¹ and 17.5 eu, respectively. These activation parameters are consistent with the desolvation that takes place in the reaction of $[\text{Cu}(\text{tet a})(\text{OH})(\text{blue})]^+$ with free hydroxide ion.

Introduction

The extreme kinetic inertness and very high thermodynamic stability of tetraamine macrocyclic ligand complexes are significant for inorganic stereochemistry,¹ since they greatly

enhance the number of potentially isolable isomers.² Thus, these complexes provide stimulating examples for studying

(1) Cabiness, D. K.; Margerum, D. W. *J. Am. Chem. Soc.* **1969**, *91*, 6540; **1970**, *92*, 2151.

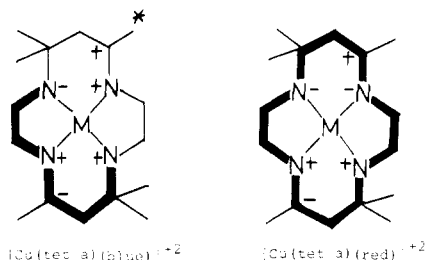
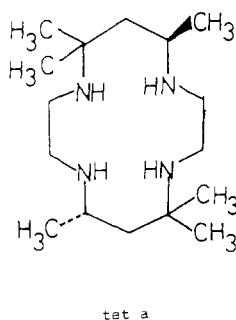


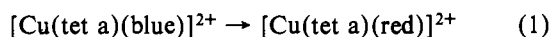
Figure 1. Structures of $[\text{Cu}(\text{tet a})(\text{blue})]^{2+}$ and $[\text{Cu}(\text{tet a})(\text{red})]^{2+}$. A plus sign at an asymmetric center indicates that the hydrogen atom of the center is above the plane of the macrocycle, and a minus sign, that it is below. Gauche conformations of the five-membered chelate rings and chair conformations of the six-membered chelate rings are indicated by heavier lines. The axial C(7) methyl group is indicated with an asterisk.

stereochemical changes.³ In aqueous solution, *meso*-5,5,7,12,12,14-hexamethyl-1,4,8,11-tetraazacyclotetradecane, tet a, reacts with copper(II) to form initially a blue complex,



tet a

which is readily converted into the more thermodynamically stable red isomer. The kinetics of blue-to-red interconversion of $[\text{Cu}(\text{tet a})]^{2+}$ (eq 1) have recently been reported.^{4,5}



In this reaction, structures have been determined for the crystalline forms of the reactant and of the product (Figure 1).⁶ As shown in Figure 1, the blue species of $[\text{Cu}(\text{tet a})]^{2+}$ differs from the red species in the configuration of a single asymmetric nitrogen center, and this nitrogen must be inverted during the blue-to-red reaction. The red species of $[\text{Cu}(\text{tet a})]^{2+}$ is more stable than the blue isomer by a factor of 10^8 ,¹ and all of the blue isomer of $[\text{Cu}(\text{tet a})]^{2+}$ converts into the red form in basic solution. Two pathways of this blue-to-red reaction, protonation pathway and coordinated-base pathway, have been proposed in our previous papers.^{4,5} In strongly acidic media, this reaction is acid catalyzed due to the required cleavage of the copper–nitrogen bond.⁵ In basic media, the blue-to-red reaction is much faster than the rates of dissociation of the macrocyclic ligand from copper(II). Hence, there is no doubt that the configurational conversion occurs while the macrocyclic ligand is coordinated. In neutral or slightly basic media, the main reaction pathway of this reaction is via a hydroxide ion that is coordinated to the copper.⁴ The coordinated hydroxide ion is so reactive that the free hydroxide ion does not contribute to the observed rate even at pH 12.⁴

In the current investigation, we have extended our study of this blue-to-red reaction to the highly basic region. Under

Table I. Apparent Molar Absorptivities at 650 nm for the $[\text{Cu}(\text{tet a})(\text{blue})]^{2+}-\text{OH}^-$ System as a Function of Hydroxide Ion Concentration at $25.0 \pm 0.1^\circ\text{C}$ and $\mu = 5.0 \text{ M}$ ($\text{NaNO}_3 + \text{NaOH}$)^a

$10^2[\text{OH}^-]$, M	ϵ_{app} , $\text{M}^{-1}\text{cm}^{-1}$	$10^2[\text{OH}^-]$, M	ϵ_{app} , $\text{M}^{-1}\text{cm}^{-1}$
6.67	141	1.80	149
4.21	149	8.41	183
2.71	158	2.44	200

^a Conditions: $[[\text{Cu}(\text{tet a})(\text{blue})]^{2+}] = 8.31 \times 10^{-4} \text{ M}$; wavelength 650 nm.

these conditions, a third type of pathway, in which the blue-to-red reaction is catalyzed by free base, contributes to the observed rate. Thus, this reaction provides an interesting example for comparing the effects of coordinated base with those of free base in the configuration inversion at the asymmetric nitrogen center.

Experimental Section

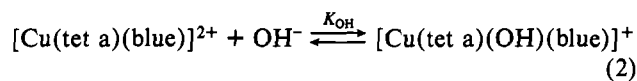
Reagents. The macrocyclic ligand tet a was prepared by using the procedure described by Hay, Lawrance, and Curtis.⁷ $[\text{Cu}(\text{tet a})(\text{blue})](\text{ClO}_4)_2$ was prepared by using the procedure described by Hay and Clark.⁸ This complex has a band maximum at 650 nm with an ϵ value of $210 \text{ M}^{-1}\text{cm}^{-1}$. Anal. Calcd for $\text{CuC}_{16}\text{H}_{36}\text{N}_4\text{Cl}_2\text{O}_8$: C, 35.13; H, 6.59; N, 10.25; Cl, 12.99. Found: C, 35.33; H, 6.72; N, 10.23; Cl, 12.90. $[\text{Cu}(\text{tet a})(\text{red})](\text{ClO}_4)_2$ was prepared by the procedure given by Cabiness.⁹ This complex has a band maximum at 512 nm with an ϵ value of $135 \text{ M}^{-1}\text{cm}^{-1}$. Anal. Calcd: C, 35.13; H, 6.59; N, 10.25; Cl, 12.99. Found: C, 34.98; H, 6.66; N, 10.37; Cl, 13.00. All other chemicals used in this work were of GR grade from Merck.

Instrumentation. A Cary 17 spectrophotometer with a thermostated cell compartment was used to measure absorption spectra and to follow the slow reactions. Rate data for faster reactions were obtained by using a Union Giken RA-401 stopped-flow spectrophotometer equipped with a Union RA-415 rapid-scan attachment. The rate constants and equilibrium constants were obtained by a linear least-squares fit of the data by using the Apple II minicomputer or the CDC Cyber-172 computer.

Kinetic Measurements. All reactions were measured at 650 nm and studied under conditions that were first order in the blue form of the copper complex. Plots of $\ln(A - A_\infty)$ vs. time were linear and gave the k_{obsd} values reported. The A_∞ values for the absorbance were measured after 10 half-lives. The average percent standard deviation for rate constants from individual runs is $\pm 2\%$ for k_{obsd} .

Results and Discussion

Addition of the solution of hydroxide ion to an aqueous solution of $[\text{Cu}(\text{tet a})(\text{blue})]^{2+}$ resulted in the rapid complex equilibria shown in eq 2. The equilibrium constant for this



reaction was determined by measuring the absorbance jump after stopped-flow mixing of base with $[\text{Cu}(\text{tet a})(\text{blue})]^{2+}$ solution. The apparent molar absorptivities at 650 nm were obtained by using the equation

$$\epsilon_{\text{app}} = A/lC_T \quad (3)$$

where A is the absorbance at 650 nm, l is the length of the cell (1.0 cm), and C_T is the total concentration of the copper(II) complexes, $[[\text{Cu}(\text{tet a})(\text{blue})]^{2+}] + [[\text{Cu}(\text{tet a})-$

(2) Liang, B.-F.; Chung, C.-S. *J. Chin. Chem. Soc. (Taipei)* **1979**, *26*, 93.
 (3) Liang, B.-F.; Margerum, D. W.; Chung, C.-S. *Inorg. Chem.* **1979**, *18*, 2001.
 (4) Liang, B.-F.; Chung, C.-S. *Inorg. Chem.* **1980**, *19*, 1867.
 (5) Liang, B.-F.; Chung, C.-S. *Inorg. Chem.* **1981**, *20*, 2152.
 (6) Clay, R. M.; Murray-Rust, P.; Murray-Rust, J. *J. Chem. Soc., Dalton Trans.* **1979**, 1135.

(7) Hay, R. W.; Lawrance, G. A.; Curtis, N. F. *J. Chem. Soc., Perkin Trans. 1* **1975**, 591.
 (8) Hay, R. W.; Clark, C. R. *J. Chem. Soc., Dalton Trans.* **1977**, 1148.
 (9) Cabiness, D. K. Ph.D. Thesis, Purdue University, 1970.

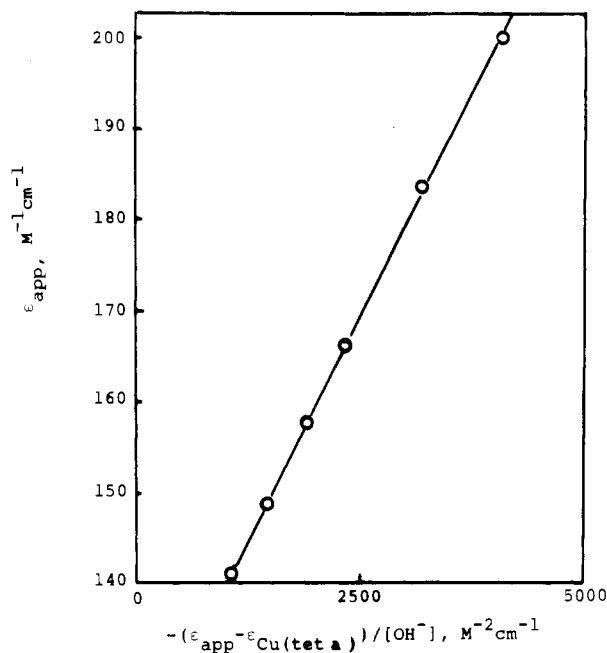


Figure 2. Spectrophotometric determination of the equilibrium constant of $[\text{Cu}(\text{tet a})(\text{blue})]^{2+}$ with hydroxide ion at 25.0 °C and $\mu = 5.0 \text{ M}$.

$(\text{OH})(\text{blue})^+$. The results are given in Table I.

According to the Rose-Drago equation (4), a plot of ϵ_{app}

$$\epsilon_{\text{app}} = \frac{-(\epsilon_{\text{app}} - \epsilon_{\text{Cu}(\text{tet a})(\text{blue})})}{K_{\text{OH}}[\text{OH}^-]} + \epsilon_{\text{Cu}(\text{tet a})(\text{OH})(\text{blue})} \quad (4)$$

against $(\epsilon_{\text{app}} - \epsilon_{\text{Cu}(\text{tet a})(\text{blue})})/[\text{OH}^-]$, where $[\text{OH}^-] = [\text{OH}^-]_{\text{T}} - [[\text{Cu}(\text{tet a})(\text{OH})(\text{blue})]^+]$, gave a straight line of slope $-1/K_{\text{OH}}$, as shown in Figure 2. Values of $[\text{OH}^-]$ were calculated by an iterative procedure in which an estimated value of K_{OH} was first used to calculate values of $[\text{OH}^-]$, which were then used to obtain a new value of K_{OH} , the operation being repeated until the least-squares deviation in the plot of ϵ_{app} vs. $(\epsilon_{\text{app}} - \epsilon_{\text{Cu}(\text{tet a})(\text{blue})})/[\text{OH}^-]$ was minimized. The value of K_{OH} thus obtained was $51.7 \pm 0.3 \text{ M}^{-1}$.

In basic solution the blue species of $[\text{Cu}(\text{tet a})]^{2+}$ converts to the thermodynamically stable red isomer, which differs from the blue isomer in the configuration of a single asymmetric nitrogen center, and this nitrogen must be inverted during the blue-to-red reaction. The observed rate constants (from a first-order dependence on the concentration of the blue form) are given in Table II. At low hydroxide ion concentration the reaction rate is directly proportional to the hydroxide ion concentration. Between $[\text{OH}^-] = 0.1 \text{ M}$ and $[\text{OH}^-] = 1.0 \text{ M}$, a limiting rate is observed. At $[\text{OH}^-]$ larger than 1.0 M, the rate again increases with the concentration of hydroxide ion as shown in Figure 3. Measurements of the absorbance jump after stopped-flow mixing of base with $[\text{Cu}(\text{tet a})(\text{blue})]^{2+}$, as well as the equilibrium study, show the existence of a hydroxide adduct to the blue form. This coordination of a hydroxide is much faster than the blue-to-red conversion. The equilibrium study indicates that the predominant form of the blue species is $[\text{Cu}(\text{tet a})(\text{blue})]^{2+}$ at low $[\text{OH}^-]$, and the concentration of $[\text{Cu}(\text{tet a})(\text{OH})(\text{blue})]^+$ increases directly in proportion to $[\text{OH}^-]$. At high $[\text{OH}^-]$ the predominant form of the blue species is $[\text{Cu}(\text{tet a})(\text{OH})(\text{blue})]^+$, and further increase of the concentration of hydroxide ion cannot increase the concentration of $[\text{Cu}(\text{tet a})(\text{OH})(\text{blue})]^+$. The pH dependence of the kinetic data shows the importance of the hydroxide adduct in the interconversion reaction. A reaction

Table II. First-Order Rate Constants for the Blue-to-Red Conversion of $[\text{Cu}(\text{tet a})]^{2+}$ as a Function of Temperature and Hydroxide Ion Concentration at $\mu = 5.0 \text{ M}$ ($\text{NaOH} + \text{NaNO}_3$)^a

temp, °C	$[\text{OH}^-], \text{M}$	$k_{\text{obsd}}, \text{s}^{-1}$	temp, °C	$[\text{OH}^-], \text{M}$	$k_{\text{obsd}}, \text{s}^{-1}$
25	1.99×10^{-4}	3.62×10^{-2}	15	4.01×10^{-2}	2.74
25	2.11×10^{-4}	4.11×10^{-2}	15	1.03	2.93
25	7.68×10^{-4}	0.147	15	2.01	3.13
25	1.38×10^{-3}	0.265	15	3.02	3.36
25	2.87×10^{-3}	0.473	15	4.05	3.58
25	8.09×10^{-3}	0.812	15	5.03	3.78
25	1.01×10^{-2}	1.67	20	4.01×10^{-2}	3.83
25	1.15×10^{-2}	1.91	20	1.03	4.22
25	1.45×10^{-2}	2.08	20	2.01	4.68
25	3.84×10^{-2}	3.18	20	3.02	5.07
25	9.10×10^{-2}	5.40	20	4.05	5.50
25	2.03×10^{-1}	5.78	20	5.03	5.86
25	4.01×10^{-1}	6.20	30	4.01×10^{-2}	7.28
25	8.07×10^{-1}	6.52	30	1.03	8.52
25	1.21	6.83	30	2.01	9.87
25	1.54	6.90	30	3.02	11.25
25	1.79	7.15	30	4.05	12.58
25	2.04	7.20	30	5.03	13.97
25	2.48	7.56	40	4.01×10^{-2}	13.78
25	3.01	8.14	40	1.03	18.16
25	3.52	8.54	40	2.01	22.80
25	4.08	8.96	40	3.02	27.48
25	4.52	9.42	40	4.05	32.10
25	5.02	9.78	40	5.03	36.79

^a Conditions: $[[\text{Cu}(\text{tet a})(\text{blue})]^{2+}]_{\text{total}} = 8.31 \times 10^{-4} \text{ M}$; wavelength 650 nm. ^b Mean value of at least three kinetic runs.

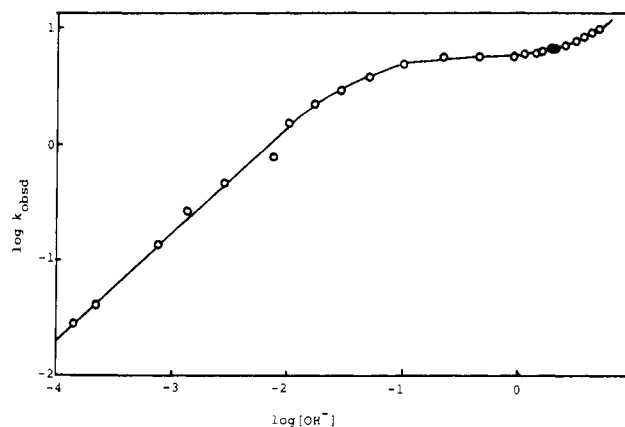
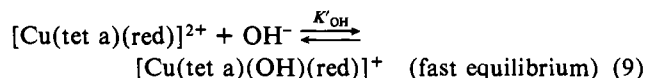
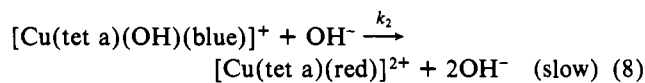
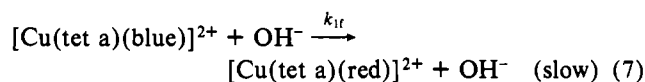
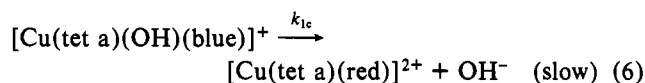
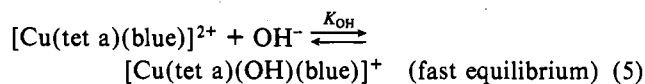


Figure 3. Rate constants for the formation of $[\text{Cu}(\text{tet a})(\text{red})]^{2+}$ from $[\text{Cu}(\text{tet a})(\text{blue})]^{2+}$ as a function of hydroxide ion concentration at 25.0 °C and $\mu = 5.0 \text{ M}$. The solid line is calculated from $k_{\text{obsd}} = (k_1 K_{\text{OH}}[\text{OH}^-] + k_2 K_{\text{OH}}[\text{OH}^-]) / (1 + K_{\text{OH}}[\text{OH}^-])$ where $k_1 = 5.51 \text{ s}^{-1}$, $k_2 = 0.84 \text{ M}^{-1} \text{ s}^{-1}$, and $K_{\text{OH}} = 51.6 \text{ M}^{-1}$; circled points are experimentally observed values.

mechanism consistent with these observations is given in eq 5–9.



The resulting rate expression is given by eq 10, where

$$-d[\text{Cu}(\text{tet a})(\text{blue})]_{\text{total}}/dt = k_{\text{obsd}}[\text{Cu}(\text{tet a})(\text{blue})]_{\text{total}} = (k_{1c}K_{\text{OH}}[\text{OH}^-] + k_{1f}[\text{OH}^-] + k_2K_{\text{OH}}[\text{OH}^-]^2) \times [\text{Cu}(\text{tet a})(\text{blue})]_{\text{total}}/(1 + K_{\text{OH}}[\text{OH}^-]) \quad (10)$$

$[\text{Cu}(\text{tet a})(\text{blue})]_{\text{total}}$ refers to the sum of $[\text{Cu}(\text{tet a})(\text{blue})]^{2+}$ and $[\text{Cu}(\text{tet a})(\text{OH})(\text{blue})]^+$.

Separate determinations of k_{1c} and k_{1f} from kinetic experiments are impossible. Letting $k_1 = k_{1c} + k_{1f}/K_{\text{OH}}$ and substituting into eq 10 give

$$k_{\text{obsd}} = (k_1K_{\text{OH}}[\text{OH}^-] + k_2K_{\text{OH}}[\text{OH}^-]^2)/(1 + K_{\text{OH}}[\text{OH}^-]) \quad (11)$$

At $[\text{OH}^-]$ values lower than 0.1 M, $k_1K_{\text{OH}}[\text{OH}^-]$ is much larger than $k_2K_{\text{OH}}[\text{OH}^-]^2$, so that $k_{\text{obsd}} = k_1K_{\text{OH}}[\text{OH}^-]/(1 + K_{\text{OH}}[\text{OH}^-])$. The reciprocal of k_{obsd} has a linear dependence on the reciprocal of the hydroxide ion concentration in accord with eq 12 as plotted in Figure 4. The values found are k_1

$$\frac{1}{k_{\text{obsd}}} = \frac{1}{k_1} + \frac{1}{k_1K_{\text{OH}}} \frac{1}{[\text{OH}^-]} \quad (12)$$

$= 5.51 \pm 0.04 \text{ s}^{-1}$ and $K_{\text{OH}} = 51.6 \pm 0.3 \text{ M}^{-1}$. The value of K_{OH} is in excellent agreement with that obtained by spectrophotometric measurement.

In order to investigate whether the main pathway of this reaction at low $[\text{OH}^-]$ is a specific free-base-catalyzed, a general free-base-catalyzed, or a coordinated-base-catalyzed one, the kinetics of this reaction was studied in the presence of NH_3 . A reaction is said to be specific base catalyzed when it is catalyzed by the hydroxide ion but not by undissociated base. General-base catalysis is observed when all proton acceptors will catalyze a reaction by removing a proton from the substrate in the transition state. Coordinated-base-catalyzed reactions, on the other hand, are inhibited by the base containing only one lone pair. As shown in Table III, this reaction reacts more slowly in the presence of NH_3 than in its absence. The fact that the formation of $[\text{Cu}(\text{tet a})(\text{NH}_3)(\text{blue})]^{2+}$ inhibits the interconversion reaction by blocking hydroxide ion from the coordination site gives good evidence that the coordinated hydroxide ion provides the best pathway to initiate the inversion of the macrocyclic nitrogen atom at low $[\text{OH}^-]$. In addition, previous studies^{3,4} and the activation parameters reported subsequently in this paper also suggest that the main reaction pathway at low $[\text{OH}^-]$ is via the hydroxide ion that is coordinated to the copper(II).

In highly basic media, $K_{\text{OH}}[\text{OH}^-] \gg 1$, we can neglect 1 in the denominator of eq 11 and get

$$k_{\text{obsd}} = k_2[\text{OH}^-] + k_1 \quad (13)$$

Plots of k_{obsd} against $[\text{OH}^-]$ at different temperatures give straight lines as shown in Figure 5. The values of k_1 and k_2 as a function of temperature are listed in Table IV. The plot of $\ln(k_1/T)$ against $1/T$ and the plot of $\ln(k_2/T)$ against $1/T$ are shown in Figures 6 and 7, respectively. The activation parameters found are listed in Table V.

In dilute base the concentration of OH^- in the vicinity of the N-H group is greatly increased due to coordination. However, the basicity of the hydroxide ion is reduced in direct proportion to its tendency to become coordinated. If the reaction mechanism had a simple proton-transfer process as the rate-determining step, then the relative concentrations and basicities of coordinated vs. free hydroxide ion should cancel one another. Similarly, a preequilibrium step with the formation of a low concentration of the deprotonated trigonal nitrogen bonded to copper would not depend on the source of the base. The effectiveness of the coordinated base suggests a concerted process in which intramolecular hydrogen bonding,

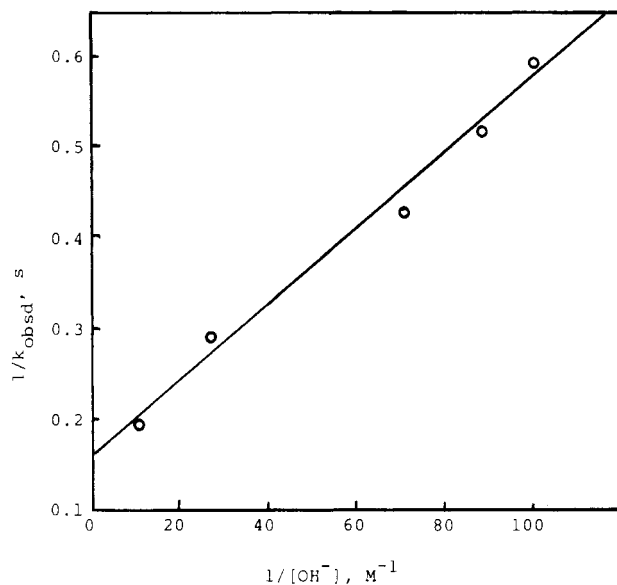


Figure 4. Double-reciprocal dependence of the observed rate constant of the blue-to-red conversion of $[\text{Cu}(\text{tet a})]^{2+}$ and the concentration of hydroxide ion at 25.0 °C and $\mu = 5.0 \text{ M}$.

Table III. First-Order Rate Constants for the Blue-to-Red Conversion of $[\text{Cu}(\text{tet a})]^{2+}$ as a Function of Hydroxide Ion Concentration at $25.0 \pm 0.1 \text{ }^\circ\text{C}$ and $\mu = 5.0 \text{ M}$ ($\text{NaOH} + \text{NaNO}_3$)^a

$[\text{OH}^-], \text{M}$	$[\text{NH}_3], \text{M}$	$k_{\text{obsd}}, \text{s}^{-1}$ ^b	$[\text{OH}^-], \text{M}$	$[\text{NH}_3], \text{M}$	$k_{\text{obsd}}, \text{s}^{-1}$ ^b
2.31×10^{-3}	0	0.42	8.81×10^{-3}	0	1.45
2.31×10^{-3}	1.0	0.11	8.81×10^{-3}	1.0	0.38
4.14×10^{-3}	0	0.68	1.02×10^{-2}	0	1.62
4.14×10^{-3}	1.0	0.19	1.02×10^{-2}	1.0	0.43
6.33×10^{-3}	0	0.87	1.30×10^{-2}	0	1.98
6.33×10^{-3}	1.0	0.28	1.30×10^{-2}	1.0	0.55

^a Conditions: $[\text{Cu}(\text{tet a})(\text{blue})]^{2+} = 8.31 \times 10^{-4} \text{ M}$; wavelength 650 nm. ^b Mean value of at least three kinetics runs.

Table IV. Rate Constants for the Coordinated-Base-Catalyzed Pathway (k_1) and the Free-Base-Catalyzed Pathway (k_2) of the Conversion of $[\text{Cu}(\text{tet a})(\text{OH})(\text{blue})]^+$ as a Function of Temperature at $\mu = 5.0 \text{ M}$ ($\text{NaOH} + \text{NaNO}_3$)

temp, °C	k_1, s^{-1}	$k_2, \text{M}^{-1} \text{s}^{-1}$	temp, °C	k_1, s^{-1}	$k_2, \text{M}^{-1} \text{s}^{-1}$
15.0	2.73	0.22	30.0	7.20	1.35
20.0	3.82	0.42	40.0	13.54	4.65
25.0	5.51	0.84			

Table V. Activation Parameters for the Configurational Conversion of $[\text{Cu}(\text{tet a})(\text{OH})(\text{blue})]^+$ at 25.0 °C and $\mu = 5.0 \text{ M}$ ($\text{NaNO}_3 + \text{NaOH}$)

$$\Delta H_1^\ddagger = 10.8 \pm 0.5 \text{ kcal/mol} \quad \Delta S_1^\ddagger = -19.0 \pm 1.2 \text{ eu}$$

$$\Delta H_2^\ddagger = 22.8 \pm 0.8 \text{ kcal/mol} \quad \Delta S_2^\ddagger = 17.5 \pm 0.8 \text{ eu}$$

nitrogen inversion, and ring conformational changes occur. The copper-bound hydroxide ion is adjacent to the N-H group, and it can react via a hydrogen-bonded chelate ring to assist the partial removal of a hydrogen from nitrogen as shown in Figure 8. The hydrogen-bonded ring structure may be important in helping to maintain the activated species long enough to permit the macrocyclic rings to twist and the nitrogen to attract a proton from a solvent molecule on the opposite site, thus leading to the inversion. In view of the solvation and hydrogen bonds formed in the activated complex for the coordinated-base pathway as shown in Figure 8, we would expect a very low ΔH^\ddagger and a negative ΔS^\ddagger for this pathway. The values of ΔH_1^\ddagger and ΔS_1^\ddagger , listed in Table V, indicate the main pathway at low $[\text{OH}^-]$ is via the hydroxide ion that is coordinated to the copper(II).

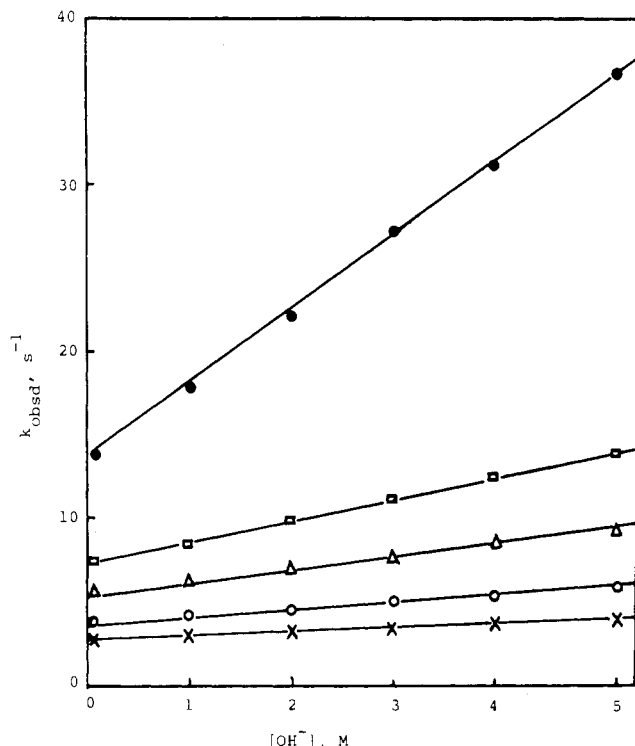


Figure 5. Plot of eq 11 to resolve the rate constants k_1 and k_2 : (●) at 40.0 °C; (□) at 30.0 °C; (Δ) at 25.0 °C; (○) at 20.0 °C; (×) at 15.0 °C.

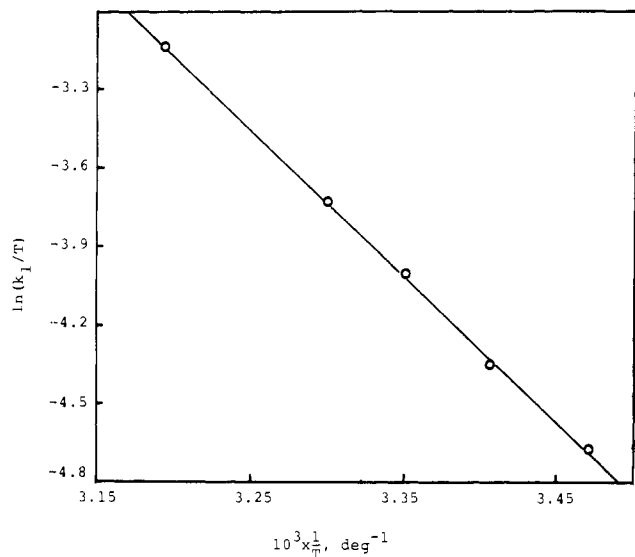


Figure 6. Graphical resolution of the activation parameters for the coordinated-base-catalyzed pathway of the blue-to-red conversion of $[\text{Cu}(\text{tet } a)(\text{OH})(\text{blue})]^+$ at $\mu = 5.0 \text{ M}$.

As shown in Table V, the large ΔH_2^\ddagger and the large positive ΔS_2^\ddagger values for the free-base-catalyzed pathway are in marked contrast to the small ΔH_1^\ddagger and the large negative ΔS_1^\ddagger values. The large ΔH_2^\ddagger and the large positive ΔS_2^\ddagger for the free-base-catalyzed pathway are consistent with the desolvation step, which occurs in the reaction of free hydroxide ion with the blue copper(II) complex. On the other hand, the coordinated-base-catalyzed pathway requires water molecules to reach the transition state as shown in Figure 8. The values of the activation parameters given in Table V reflect the desolvation and solvation that take place in the reactions with free hydroxide ion and coordinated hydroxide ion, respectively.

Since 1966, many transition-metal complexes containing open-chain amines have been resolved into their optical enantiomorphs, and the kinetics of inversion and proton exchange

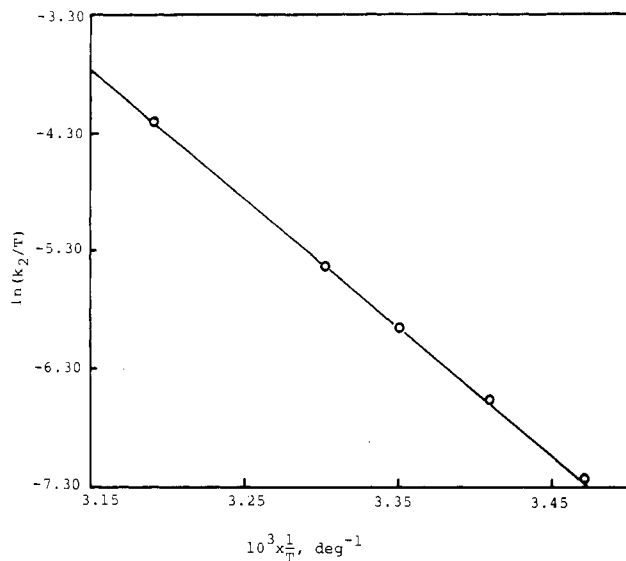


Figure 7. Graphical resolution of the activation parameters for the free-base-catalyzed pathway of the blue-to-red conversion of $[\text{Cu}(\text{tet } a)(\text{OH})(\text{blue})]^+$ at $\mu = 5.0 \text{ M}$.

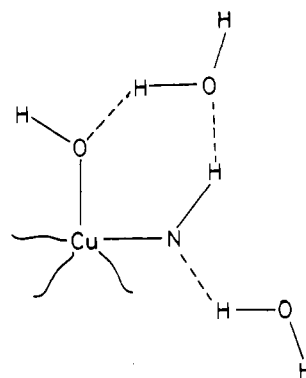


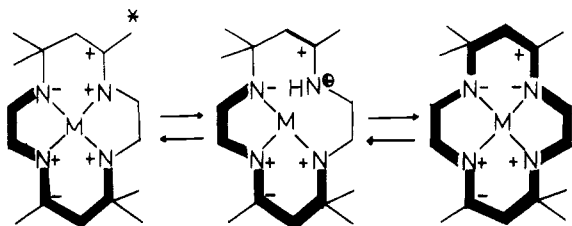
Figure 8. Proposed intramolecular proton transfer and concerted inversion of nitrogen in $[\text{Cu}(\text{tet } a)(\text{OH})(\text{blue})]^+$.

at asymmetric nitrogen centers in these complexes have been studied.¹⁰⁻²⁵ The rates of inversion and proton exchange are both second order: first order in $[\text{OH}^-]$ and first order in the concentration of metal complex. The retention ratios for these reactions are very large, implying that the configuration about the N atom is retained most of the time that the proton is off the quaternary N site.²⁶ The kinetics results for the proton

- (10) Buckingham, D. A.; Marzilli, P. A.; Sargeson, A. M. *Inorg. Chem.* **1967**, *6*, 1032.
- (11) Buckingham, D. A.; Marzilli, L. G.; Sargeson, A. M. *J. Am. Chem. Soc.* **1967**, *89*, 825.
- (12) Buckingham, D. A.; Marzilli, L. G.; Sargeson, A. M. *J. Am. Chem. Soc.* **1967**, *89*, 3428.
- (13) Buckingham, D. A.; Marzilli, L. G.; Sargeson, A. M. *Inorg. Chem.* **1968**, *7*, 915.
- (14) Buckingham, D. A.; Marzilli, L. G.; Sargeson, A. M. *J. Am. Chem. Soc.* **1968**, *90*, 6028.
- (15) Buckingham, D. A.; Marzilli, P. A.; Sargeson, A. M. *Inorg. Chem.* **1969**, *8*, 1595.
- (16) Buckingham, D. A.; Marzilli, L. G.; Sargeson, A. M. *J. Am. Chem. Soc.* **1969**, *91*, 5227.
- (17) Buckingham, D. A.; Dwyer, M.; Sargeson, A. M.; Watson, K. J. *Acta Chem. Scand.* **1972**, *26*, 2813.
- (18) Erickson, L. E.; Dappen, A. J.; Uhlenhopp, J. C. *J. Am. Chem. Soc.* **1969**, *91*, 2510.
- (19) Erickson, L. E.; Fritz, H. L.; May, R. J.; Wright, D. A. *J. Am. Chem. Soc.* **1969**, *91*, 2513.
- (20) Erickson, L. E. *J. Am. Chem. Soc.* **1969**, *91*, 6284.
- (21) Goddard, J. B.; Basolo, F. *Inorg. Chem.* **1969**, *8*, 2223.
- (22) Haake, P.; Turley, P. C. *J. Am. Chem. Soc.* **1968**, *90*, 2293.
- (23) Halpern, B. A.; Sargeson, M.; Turnbull, K. B. *J. Am. Chem. Soc.* **1966**, *88*, 4630.
- (24) Pitner, T. P.; Martin, R. B. *J. Am. Chem. Soc.* **1971**, *93*, 4400.
- (25) Searle, G. H.; Keene, F. R. *Inorg. Chem.* **1972**, *11*, 1006.

Table VI. Activation Parameters for Inversions at Asymmetric Nitrogen Centers in Metal Complexes

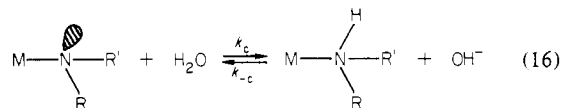
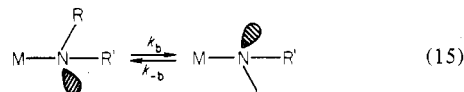
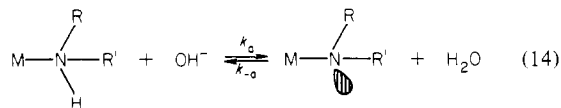
complex	temp, °C	ΔH^\ddagger , kcal/mol	ΔS^\ddagger , eu	ref
$[\text{Co}(\text{NH}_3)_4(\text{sar})]^{2+}$	34.3	18.6	21	15
$[\text{Co}(\text{NH}_3)_4(N\text{-Meen})]^{3+}$	34.3	23.8	30	11
<i>trans,trans</i> - $[\text{Co}(\text{NO}_2)_2(N\text{-Meen})_2]^+$	34.3	28.4	34	12
$[\text{Pt}(N\text{-Meen})(\text{NH}_3)_2]^{2+}$	25.0	19.2	17	21
$[\text{Pt}(N\text{-Meen})(\text{phen})]^{2+}$	25.0	16.7	17	21
<i>trans</i> - $[\text{Co}(\text{dien})_2]^{3+}$	34.9	23.5	29	25
<i>syn</i> - $[\text{Co}(\text{trenen})\text{N}_3]^{2+}$	34	22.7	28	25

**Figure 9.** Configuration conversions of $[\text{Cu}(\text{tet a})(\text{blue})]^{2+}$ in strongly acidic media (key as in Figure 1).

exchanges and the nitrogen inversions of these complexes are consistent with the formation of a common intermediate as shown by eq 14-16.

Step 1 (k_a) leads to proton exchange. The rate constant of reprotonation (k_{-a}) is very large, much larger than the actual rate constant of inversion of the amide complex (k_b), resulting largely in retention of configuration. The activation parameters for the racemizations of these complex are listed in Table VI. The ΔS_2^\ddagger value for the free-base-catalyzed pathway of the blue-to-red interconversion of $[\text{Cu}(\text{tet a})(\text{OH})]^{2+}$ is very similar to those listed in this table, suggesting the mechanism

(26) Wilkins, R. G. "The Study of Kinetics and Mechanism of Reactions of Transition Metal Complexes"; Allyn and Bacon: Boston, MA, 1974; pp 354-357.



for the free-base-catalyzed pathway of the reaction of $[\text{Cu}(\text{tet a})(\text{OH})(\text{blue})]^{2+}$ is the same as that shown by this scheme (eq 14-16).

It is interesting to compare the ΔH^\ddagger values for the reactions of the open-chain-ligand complexes given in Table VI and that for the free-base reaction of $[\text{Cu}(\text{tet a})(\text{OH})(\text{blue})]^{2+}$. The racemization of each of these open-chain-ligand complexes needs to invert only one stable chelate ring; the ΔH^\ddagger values are in the range of 16.7-28.4 kcal/mol compared to a ΔH_2^\ddagger value of 22.8 kcal/mol for $[\text{Cu}(\text{tet a})(\text{OH})(\text{blue})]^{2+}$, which has to invert two adjacent unstable chelate rings.

There are three types of pathways for the blue-to-red interconversion of $[\text{Cu}(\text{tet a})]^{2+}$ found under different conditions. In basic media, both coordinated-base-catalyzed and free-base-catalyzed pathways contribute to the observed rate. In strongly acidic media, this reaction is acid catalyzed due to the required cleavage of the copper-nitrogen bond.⁵ This protonation pathway is shown in Figure 9.

Acknowledgment. We are grateful to the Chemistry Research Center, National Science Council of the Republic of China, for financial support. We are also grateful to the Chun-Sun Institute of Science and Technology of the Republic of China for elemental analyses and for providing laboratory facilities.

Registry No. OH^- , 14280-30-9.

Contribution from the Department of Chemistry, Clemson University, Clemson, South Carolina 29631

Some Reactions of Sulfonyl Hypohalites with Sulfur Tetrafluoride

BRIAN A. O'BRIEN and DARRYL D. DESMARTEAU*

Received March 30, 1983

The reactions of ClOSO_2F , BrOSO_2F , and $\text{ClOSO}_2\text{CF}_3$ with SF_4 have been investigated. It has been found that the reactions proceed to form either trifluorosulfonium salts or covalent adducts. In the cases where the hypochlorites were used, the unusual cation SF_4Cl^+ can be postulated as a reactive intermediate. Characterizations of the new compounds $\text{SF}_3^+\text{FSO}_3^-$, $\text{SF}_3^+\text{CF}_3\text{SO}_3^-$, *cis*- $\text{SF}_4(\text{Cl})\text{OSO}_2\text{F}$, *trans*- $\text{SF}_4(\text{Cl})\text{OSO}_2\text{F}$, and *trans*- $\text{SF}_4(\text{Cl})\text{OSO}_2\text{CF}_3$ are reported. The SF_3^+ salts are thermally unstable, decomposing to SF_4 , SOF_2 , and $(\text{XSO}_2)_2\text{O}$ ($\text{X} = \text{F}, \text{CF}_3$).

Introduction

The sulfonyl hypohalites are a class of compounds whose great oxidizing power and electrophilicity allow them to participate in a number of unique and interesting reactions.^{1,2} For example, bromine(I) and Chlorine(I) fluorosulfate²⁻⁴ and

chlorine(I) and bromine(I) trifluoromethanesulfonate⁴⁻⁶ have been shown to react with various covalent organic and inorganic halides to yield the corresponding sulfonic acid derivatives. These compounds have also been shown to add readily

(1) Aubke, F.; DesMarteau, D. D. *Fluorine Chem. Rev.* **1977**, *8*, 73.
 (2) Schack, C. J.; Christe, K. O. *Isr. J. Chem.* **1978**, *17*, 20.
 (3) DesMarteau, D. D. *Inorg. Chem.* **1968**, *7*, 434.

(4) Johri, K. K.; Katsuhara, Y.; DesMarteau, D. D. *J. Fluorine Chem.* **1982**, *19*, 227.
 (5) Katsuhara, Y.; Hammaker, R. M.; DesMarteau, D. D. *Inorg. Chem.* **1980**, *19*, 607.
 (6) Katsuhara, Y.; DesMarteau, D. D. *J. Am. Chem. Soc.* **1980**, *102*, 2681.